

Addition of Isocyanides at Diiron μ -Vinyliminium Complexes: Synthesis of Novel Ketenimine–Bis(alkylidene) Complexes

Luigi Busetto,[†] Fabio Marchetti,^{‡,§} Stefano Zacchini,[†] and Valerio Zanotti^{*,†}

Dipartimento di Chimica Fisica e Inorganica, Università di Bologna, Viale Risorgimento 4, 40136 Bologna, Italy, and Dipartimento di Chimica e Chimica Industriale, Università di Pisa, Via Risorgimento 35, I-56126 Pisa, Italy

Received May 15, 2008

Reactions of the vinyliminium complexes $[\text{Fe}_2\{\mu\text{-}\eta^1\text{:}\eta^3\text{-C}_\gamma(\text{R}')\text{C}_\beta(\text{H})\text{C}_\alpha\text{N}(\text{Me})(\text{R})\}(\mu\text{-CO})(\text{CO})(\text{Cp})_2]\text{[SO}_3\text{CF}_3]$ ($\text{R} = \text{Xyl}$, $\text{R}' = \text{Me}$, **1a**; $\text{R} = \text{Xyl}$, $\text{R}' = \text{CO}_2\text{Me}$, **1b**; $\text{R} = 4\text{-C}_6\text{H}_4\text{OMe}$, $\text{R}' = \text{CO}_2\text{Me}$, **1c**; $\text{Xyl} = 2,6\text{-Me}_2\text{C}_6\text{H}_3$) with isocyanides (CNR''), in the presence of NaH, lead to abstraction of the $\text{C}_\beta\text{-H}$ proton and to isocyanide addition with formation of a carbon–carbon double bond. The observed products are the ketenimine–bis(alkylidene) complexes $[\text{Fe}_2\{\mu\text{-}\eta^1\text{:}\eta^2\text{-C}_\gamma(\text{R}')\text{C}_\beta(\text{CNR}'')\text{C}_\alpha\text{N}(\text{Me})(\text{R})\}(\mu\text{-CO})(\text{CO})(\text{Cp})_2]$ ($\text{R} = \text{Xyl}$, $\text{R}' = \text{Me}$, $\text{R}'' = \text{Xyl}$, **2a**; $\text{R} = \text{Xyl}$, $\text{R}' = \text{CO}_2\text{Me}$, $\text{R}'' = \text{Xyl}$, **2b**; $\text{R} = \text{Xyl}$, $\text{R}' = \text{CO}_2\text{Me}$, $\text{R}'' = \text{Bu}^t$, **2c**; $\text{R} = \text{Xyl}$, $\text{R}' = \text{CO}_2\text{Me}$, $\text{R}'' = 4\text{-C}_6\text{H}_4\text{CN}$, **2d**; $\text{R} = 4\text{-C}_6\text{H}_4\text{OMe}$, $\text{R}' = \text{CO}_2\text{Me}$, $\text{R}'' = \text{Bu}^t$, **2e**), obtained in 60–70% yields. Conversely, the vinyliminium complex $[\text{Fe}_2\{\mu\text{-}\eta^1\text{:}\eta^3\text{-C}_\gamma(\text{CO}_2\text{Me})\text{C}_\beta(\text{H})\text{C}_\alpha\text{N}(\text{Me})_2\}(\mu\text{-CO})(\text{CO})(\text{Cp})_2]\text{[SO}_3\text{CF}_3]$ (**1d**) undergoes double isocyanide addition. Reactions of **1d** with a 2-fold excess of CNXyl or CNBu^t , in the presence of NaH, afford $[\text{Fe}(\text{CO})(\text{Cp})\text{C}_\alpha(\text{NMe}_2)\text{C}_\beta(\text{CNXyl})\text{C}_\gamma(\text{CO}_2\text{Me})\text{C}(\text{NXyl})\text{Fe}(\text{CO})(\text{Cp})]$ (**3**) and $[\text{Fe}(\text{CO})(\text{Cp})\text{C}(\text{NBu}^t)\text{C}_\alpha(\text{NMe}_2)\text{C}_\beta\text{C}_\gamma(\text{CO}_2\text{Me})\text{Fe}(\text{Cp})(\text{CO})\text{CNBu}^t]$ (**4**), respectively. Finally, the vinyliminium complex $[\text{Fe}_2\{\mu\text{-}\eta^1\text{:}\eta^3\text{-C}_\gamma(\text{H})\text{C}_\beta(\text{H})\text{C}_\alpha\text{N}(\text{Me})_2\}(\mu\text{-CO})(\text{CO})(\text{Cp})_2]\text{[SO}_3\text{CF}_3]$ (**1e**), treated with CNBu^t and NaH, yields a mixture of the diiron aminocarbene complexes $[\text{Fe}_2\{\mu\text{-CN}(\text{Me})_2\}(\mu\text{-CO})(\text{CO})(\text{Cp})(\text{C}_5\text{H}_5\text{CH}_2\text{CN})(\text{CNBu}^t)]$, (**6**) and $[\text{Fe}_2\{\mu\text{-CN}(\text{Me})_2\}(\mu\text{-CO})(\text{CO})(\text{Cp})_2(\text{CNBu}^t)]$ (**5**). The molecular structures of **2a,b**, **3**·1.5 CH_2Cl_2 , **4**, and **6**·0.5 Et_2O have been ascertained by X-ray diffraction studies.

Introduction

Bridging organic fragments, in dinuclear complexes, often display unique reactivity patterns, distinct from those observed in monometallic complexes. Activation effects provided by multisite coordination have been exploited to accomplish transformations of bridging hydrocarbyl ligands otherwise unattainable,¹ which are of potential interest in metal-assisted organic synthesis and catalysis.² Our interest in the topic has been centered on the chemistry of the diiron μ -vinyliminium complexes $[\text{Fe}_2\{\mu\text{-}\eta^1\text{:}\eta^3\text{-C}_\gamma(\text{R}')\text{C}_\beta(\text{H})\text{C}_\alpha\text{N}(\text{Me})(\text{R})\}(\mu\text{-CO})(\text{CO})(\text{Cp})_2]\text{[SO}_3\text{CF}_3]$ (**1**; $\text{R}' = \text{alkyl}$, aryl ; $\text{R} = \text{Me}$, CH_2Ph , Xyl ; $\text{Xyl} = 2,6\text{-Me}_2\text{C}_6\text{H}_3$) (Scheme 1),³ which combine activation effects due to the bridging coordination with those provided by the presence of an iminium functionality.⁴ The overall result is a remarkable reactivity toward nucleophiles (NaBH_4 ,⁵ CN^- ,⁶

* To whom correspondence should be addressed. E-mail: valerio.zanotti@unibo.it.

[†] Università di Bologna.

[‡] Università di Pisa.

[§] Fabio Marchetti, born in 1974 in Bologna, Italy.

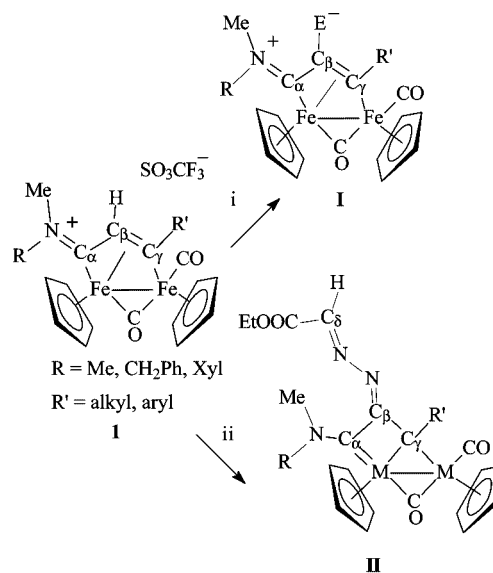
(1) Ritleng, V.; Chetcuti, M. J. *Chem. Rev.* **2007**, *107*, 797.

(2) (a) Braunstein, P.; Rosè, J. In *Metal Clusters in Chemistry*; Braunstein, P., Oro, L. A., Raithby P. R., Eds.; Wiley-VCH: Weinheim, Germany, 1999; p 616. (b) *Catalysis by Di- and Polynuclear Metal Cluster Complexes*; Adams, R. A., Cotton, F. A., Eds.; Wiley-VCH: New York, 1998. (c) Adams, R. D.; Captain, B. J. *Organomet. Chem.* **2004**, *689*, 4521. (d) Van Den Beuken, E. K.; Feringa, B. L. *Tetrahedron* **1998**, *54*, 12985. (e) Severin, K. *Chem. Eur. J.* **2002**, *8*, 1514. (f) Cowie, M. *Can. J. Chem.* **2005**, *83*, 1043.

(3) (a) Albano, V. G.; Busetto, L.; Marchetti, F.; Monari, M.; Zacchini, S.; Zanotti, V. *Organometallics* **2003**, *22*, 1326. (b) Albano, V. G.; Busetto, L.; Marchetti, F.; Monari, M.; Zacchini, S.; Zanotti, V. *J. Organomet. Chem.* **2004**, *689*, 528.

(4) Erkkilä, A.; Majander, I.; Pihko, P. M. *Chem. Rev.* **2007**, *107*, 5416.

Scheme 1



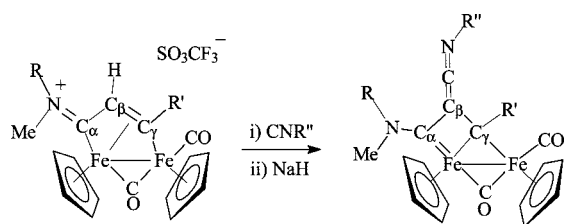
i: NaH/Me₃NO, NaH/S₈, NaH/Se (E = O, S, Se);

ii: NaH, N₂CH(COOEt)

and acetylides⁷) with the observation of unconventional reaction patterns. Indeed, instead of the usual 1,4-conjugated addition (Michael type nucleophilic addition), attacks at the bridging vinyliminium ligand are directed to the iminium carbon (C_α) or to the adjacent position (C_β).

Another very effective route to the transformation and functionalization of the bridging vinyliminium ligands is based upon the removal of the $\text{C}_\beta\text{-H}$ proton, generating a reactive

Scheme 2



	R	R'	R''	
1a	Xyl	Me	Xyl	2a
1b	Xyl	CO ₂ Me	Xyl	2b
1b	Xyl	CO ₂ Me	Bu ¹	2c
1b	Xyl	CO ₂ Me	<i>p</i> -CN-C ₆ H ₄	2d
1c	<i>p</i> -OMe-C ₆ H ₄	CO ₂ Me	Bu ¹	2e

intermediate, which can be “trapped” with appropriate reagents.⁸ Examples are the reactions with group 16 elements, affording the zwitterionic complexes **I** (Scheme 1),⁹ and those with diazoacetates, leading to the formation of the azine–bis(alkylidene) complexes **II** (Scheme 1).¹⁰

The transformations of **I** are accompanied and made possible by changes in the coordination mode of the rather flexible C₃-bridged organic frame. Indeed, **I** can be regarded as a vinyliminium or amino–allylidene complex, whereas **II** is better described as a bis(alkylidene) compound.

We now report studies on the reactions of the deprotonated vinyliminium complexes with isocyanides, aimed at introducing new functionalities on the central carbon atom of the C₃ bridging frame. Isocyanides appear to be good candidates for these investigations, in that they are very reactive species toward transition-metal complexes and can act through a broad variety of mechanisms, including ligand addition or substitution and migratory insertion. Moreover, addition of isocyanides to bridging unsaturated C₃ hydrocarbonyl ligands (allenyls) are known.¹¹

Results and Discussion

Isocyanide Addition at the Bridging Vinyliminium Ligand.

The μ -vinyliminium diiron complexes **1a–c** react with isocyanides (CNR'') in THF solution, in the presence of NaH, affording the corresponding ketenimine–bis(alkylidene) complexes **2a–e** (Scheme 2). The reaction consists of the C _{β} –H deprotonation and addition of the isocyanide at the C _{β} position, with formation of a carbon–carbon double bond.

Compounds **2a–e** have been obtained in about 60–70% yield, after purification by column chromatography on alumina, and characterized by IR and NMR spectroscopy and elemental analysis. Moreover, the molecular structures of **2a,b** have been

(5) (a) Albano, V. G.; Busetto, L.; Marchetti, F.; Monari, M.; Zacchini, S.; Zanotti, V. *Organometallics* **2004**, *23*, 3348. (b) Albano, V. G.; Busetto, L.; Marchetti, F.; Monari, M.; Zacchini, S.; Zanotti, V. *J. Organomet. Chem.* **2005**, *690*, 837.

(6) Albano, V. G.; Busetto, L.; Marchetti, F.; Monari, M.; Zacchini, S.; Zanotti, V. *J. Organomet. Chem.* **2006**, *691*, 4234.

(7) Busetto, L.; Marchetti, F.; Zacchini, S.; Zanotti, V. *Eur. J. Inorg. Chem.* **2007**, 1799.

(8) Busetto, L.; Marchetti, F.; Zacchini, S.; Zanotti, V. *Organometallics* **2005**, *24*, 2297.

(9) Busetto, L.; Marchetti, F.; Zacchini, S.; Zanotti, V. *Organometallics* **2006**, *25*, 4808.

(10) Busetto, L.; Marchetti, F.; Zacchini, S.; Zanotti, V. *Organometallics* **2007**, *26*, 3577.

(11) (a) Doherty, S.; Hogarth, G.; Waugh, M.; Scanlan, T. H.; Clegg, W.; Elsegood, M. R. J. *Organometallics* **1999**, *18*, 3178. (b) Cherkas, A. A.; Hadj-Bagheri, N.; Carty, A. J.; Sappa, E.; Pellinghelli, M. V.; Tiripicchio, A. *Organometallics* **1990**, *9*, 1887.

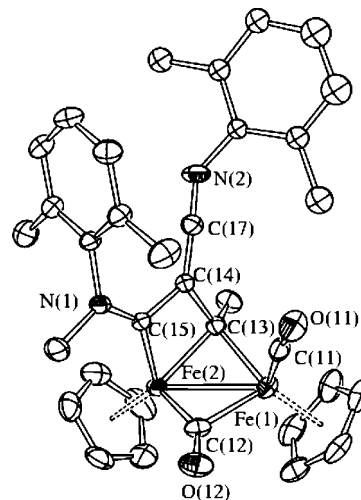


Figure 1. Molecular structure of **2a**, with key atoms labeled. Displacement ellipsoids are shown at the 30% probability level. All H atoms have been omitted for clarity. Only the main image of the disordered Xyl bound to N(2) is depicted.

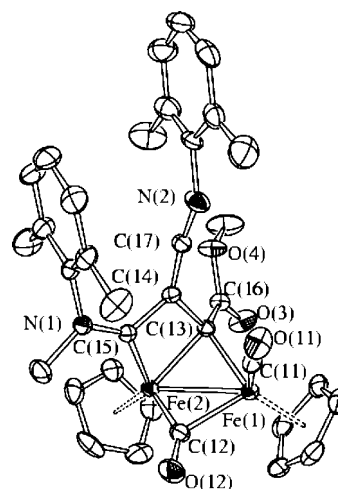


Figure 2. Molecular structure of **2b**, with key atoms labeled. Displacement ellipsoids are shown at the 30% probability level. All H atoms have been omitted for clarity. Only the main image of the disordered OMe bound to C(16) is depicted.

ascertained by X-ray diffraction: the ORTEP molecular diagrams are shown in Figures 1 and 2, and relevant bond lengths and angles are reported in Table 1. The two molecules display very similar geometries and bonding parameters, and they can be viewed as being composed of a *cis*-[Fe₂(μ -CO)(CO)(Cp)₂] core to which is coordinated the ketenimine–bis(alkylidene) ligand μ - η^1 : η^2 -C _{γ} (R')C _{β} (CNR'')C _{α} N(Me)(R). The Fe(1)–C(13) (1.985(3) and 1.987(3) Å for **2a,b**, respectively), Fe(2)–C(13) (1.995(3) and 1.995(2) Å), and Fe(2)–C(15) (1.889(3) and 1.914(2) Å) interactions are typical for a bridging alkylidene (C _{γ} , C(13)) and a terminal aminocarbene (C _{α} , C(15)).^{8,12} In agreement with this, the C(15)–N(1) (1.327(4) and 1.334(3) Å) interaction displays a partial double-bond character and N(1) shows an almost perfect sp² hybridization (sums of angles 360.0(5) and 360.0(3)°). Moreover, Fe(2) and C(14) are at a nonbonding distance (2.51(2) and 2.52(2) Å), as previously found in other diiron bis(alkylidene) complexes.^{5,7} Finally, both C(14)–C(17) (1.339(4) and 1.339(3) Å) and C(17)–N(2) (1.210(4) and 1.193(3) Å) are almost pure double bonds, as expected for a ketenimine.

Table 1. Selected Bond Lengths (Å) and Angles (deg) for **2a,b**

	2a	2b
Fe(1)–Fe(2)	2.5146(9)	2.5197(7)
Fe(1)–C(11)	1.734(4)	1.741(3)
Fe(1)–C(12)	2.013(4)	2.018(3)
Fe(2)–C(12)	1.830(4)	1.840(3)
Fe(1)–C(13)	1.985(3)	1.987(2)
Fe(2)–C(13)	1.995(3)	1.995(2)
Fe(2)⋯C(14)	2.51(2)	2.52(2)
Fe(2)–C(15)	1.899(3)	1.914(2)
C(11)–O(11)	1.155(4)	1.152(3)
C(12)–O(12)	1.177(4)	1.175(3)
C(13)–C(14)	1.508(4)	1.518(3)
C(14)–C(15)	1.430(4)	1.415(3)
C(15)–N(1)	1.327(4)	1.334(3)
C(14)–C(17)	1.339(4)	1.339(3)
C(17)–N(2)	1.210(4)	1.193(3)
Fe(1)–C(13)–C(14)	117.8(2)	115.89(16)
C(13)–C(14)–C(15)	100.9(2)	100.90(19)
C(14)–C(15)–N(1)	124.9(3)	126.0(2)
C(17)–C(14)–C(15)	132.5(3)	129.7(2)
C(13)–C(14)–C(17)	126.0(3)	129.2(2)
C(14)–C(17)–N(2)	166.6(4)	168.5(3)
sum of angles at N(1)	360.0(5)	360.0(3)

The IR spectra (in CH₂Cl₂ solution) of **2a–e** exhibit the usual $\nu(\text{CO})$ band pattern consisting of two absorptions attributable to the terminal and bridging carbonyls (e.g. at 1931 and 1745 cm⁻¹ for **2c**). Moreover, the ketenimine group gives rise to a strong absorption, at about 2100–1960 cm⁻¹.

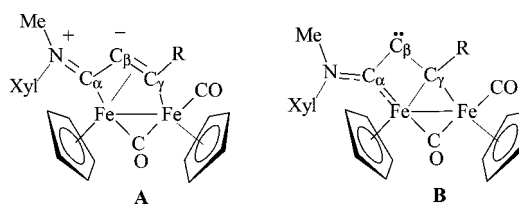
The NMR spectra of **2a–e** indicate that a single isomeric form is present in solution, in spite of the fact that several isomers are possible, in theory, due to the different orientations that the N substituents might assume as a consequence of the double-bond character of the ketenimine group and of the C_α–N interaction. NMR NOE experiments carried on **2a–d** evidenced that, in all cases, the N substituents (Me and Xyl) adopt the *E* configuration (Me pointing far from the ketenimine moiety), as found in the solid state for **2a,b**. More precisely, a significant NOE effect was observed between one Cp and the *N*-Me, whereas no enhancement was found for the methyls of the Xyl group. The observed *E* configuration was rather unexpected, since analogous vinyliminium complexes, in which C_β–H has been replaced by other groups, usually display the opposite *Z* configuration.^{3b,9,10}

Major features in the ¹³C NMR spectra are given by the C_α, C_β, and C_γ resonances, which fall in the ranges 235–243, 95–102, and 124–156 ppm, respectively, and are consistent with the values found in related diiron bis(alkylidene) complexes.¹⁰ In particular, the C_α and C_γ resonances are found in regions typical for aminocarbene and alkylidene carbons, respectively. Finally, a resonance at ca. 140 ppm is attributed to the central carbon of the ketenimine moiety.

Some aspects concerning the reaction should be pointed out. First, the C_β–H proton is removed easily, which is presumably associated with the presence of the iminium moiety. Thus, the in situ formation of a carbanion equivalent should be related to the synthetic approach used in enamine/iminium ion catalysis.^{4,13} Moreover, we have previously evidenced that the Fe–C_α

(12) (a) Allen, F. H.; Kennard, O.; Watson, D. G.; Brammer, L.; Orpen, A. G.; Taylor, R. *J. Chem. Soc., Perkin Trans.* **1987**, S1. (b) Orpen, A. G.; Brammer, L.; Allen, F. H.; Kennard, O.; Watson, D. G.; Taylor, R. *J. Chem. Soc., Dalton Trans.* **1989**, S1.

(13) (a) List, B. *Acc. Chem. Res.* **2004**, *37*, 548. (b) Mukherjee, S.; Yang, J. W.; Hoffmann, S.; List, B. *Chem. Rev.* **2007**, *107*, 5471. (c) Lelais, G.; MacMillan, D. W. C. *Aldrichim. Acta* **2006**, *39*, 79. (d) Cavill, J. L.; Elliott, R. L.; Evans, G.; Jones, I. L.; Platts, J. A.; Ruda, A. M.; Tomkinson, N. C. O. *Tetrahedron* **2006**, *62*, 410.

Scheme 3

interaction in the μ -vinyliminium species **1** displays some Fischer-type aminocarbene character,⁸ and this also helps to explain the acidic character of the C_β–H hydrogen.

A second observation concerns the nature of the intermediate species formed by deprotonation. In a previous paper, we proposed that these intermediates might assume either zwitterionic (**A**) or carbene (**B**) character (Scheme 3).⁸ The formation of the ketenimine functionality, by isocyanide addition to the C_β carbon of the vinyliminium ligand, would be better explained by assuming the carbene-like intermediate **B** (Scheme 3). Indeed, metal-assisted coupling of carbenes and isocyanides is a well-established method for generating ketenimines.

In particular, metal-assisted synthesis of ketenimines can be accomplished either by coupling of metal carbenes with isocyanides¹⁴ or from metal isocyanides and diazo compounds acting as carbene sources.¹⁵ Furthermore, in a number of cases ketenimine groups have been generated by isocyanide addition, insertion, multiple insertion, or coupling with a variety of different ligands and metal complexes, through rather unpredictable reactions.¹⁶

A final consideration concerns the potential of the ketenimine functionality in the perspective of further transformations of the bridging ligand. In theory, new highly functionalized bridging frames should be accessible by reactions involving the ketenimine functionality, which is the ideal substrate for the synthesis of heterocycles by cycloaddition reactions.¹⁷

Multiple Isocyanide Addition. The coupling between vinyliminium ligands and isocyanides shown in Scheme 2 is not general, in that other vinyliminium complexes, such as [Fe₂{ μ - η^1 : η^3 -C_γ(R')C_β(H)C_αN(Me)₂}(μ -CO)(CO)(Cp)₂][SO₃CF₃] (R' = CO₂Me (**1d**), H (**1e**), Me (**1f**), Tol (**1g**)) failed to produce ketenimine bis(alkylidene) species analogous to **2a–e**, under reaction conditions similar to those described above. The reactions investigated involved several isocyanides (CNR''; R'' = Xyl, Bu^t, *p*-CN-C₆H₄, 2,4-C₆H₃(OMe)₂, Ph, *p*-Cl-C₆H₄, CH₂SiMe₃) and generally resulted in the formation of unidentified decomposition products, with minor amounts of the compounds which are known to be generated by deprotonation of the vinyliminium complexes in the absence of trapping

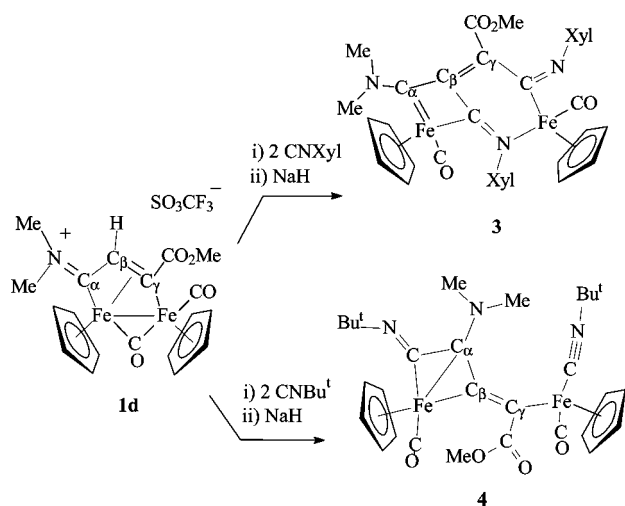
(14) (a) Fernandez, I.; Cossio, F. P.; Sierra, M. A. *Organometallics* **2007**, *26*, 3010. (b) Cadierno, V.; Garcia-Alvarez, J.; Gimeno, J.; Rubio-Garcia, J. *J. Organomet. Chem.* **2005**, *690*, 5856. (c) Aumann, R. *Angew. Chem.* **1988**, *100*, 1512.

(15) (a) Strecker, B.; Werner, H. *Angew. Chem.* **1990**, *102*, 310. (b) Yarrow, D. J.; Ibers, J. A.; Tatsuno, Y.; Otsuka, S. *J. Am. Chem. Soc.* **1973**, *95*, 8590.

(16) (a) Turculet, L.; Tilley, T. D. *Organometallics* **2002**, *21*, 3961. (b) Wu, Z.; Diminnie, J. B.; Xue, Z. *Organometallics* **1999**, *18*, 1002. (c) Scott, M. J.; Lippard, S. J. *Organometallics* **1998**, *17*, 1769. (d) Scott, M. J.; Lippard, S. J. *J. Am. Chem. Soc.* **1997**, *119*, 3411. (e) Vicente, J.; Abad, J.-A.; Shaw, K. F.; Gil-Rubio, J.; Ramirez de Arellano, M. C.; Jones, P. G. *Organometallics* **1997**, *16*, 4557. (f) Antinolo, A.; Fajardo, M.; Gil-Sanz, R.; Lopez-Mardomingo, C.; Otero, A.; Atmani, A.; Kubicki, M. M.; El Krami, S.; Mugnier, Y.; Mourad, Y. *Organometallics* **1994**, *13*, 1200. (g) Tanase, T.; Fukushima, T.; Nomura, T.; Yamamoto, Y.; Kobayashi, K. *Inorg. Chem.* **1994**, *33*, 32. (h) Wouters, J. M. A.; Klein, R. A.; Elsevier, C. J.; Zoutberg, M. C.; Stam, C. H. *Organometallics* **1993**, *12*, 3864.

(17) Alajarín, M.; Vidal, A.; Tovar, F. *Targets Heterocycl. Syst.* **2000**, *4*, 293.

Scheme 4



reagents.⁷ However, in a few cases, we have been able to identify new reaction products. As an example, the reactions of **1d** with 2 equiv of CNXyl or CNBu^t, in the presence of NaH, afforded the dinuclear compounds **3** and **4**, respectively (Scheme 4).

Complexes **3** and **4** have been identified by X-ray diffraction (Figures 3 and 4, Tables 2 and 3). The bridging ligand in **3** is unprecedented, and it can be formally considered as the result of the fusion of two rings: 1-metalla-2-aza-6-iminocyclohexa-2,4-diene (**III**) and 1-metalla-2-amino-4-iminocyclobut-1-ene (**IV**). Six-membered metallacycles of type **III** have been reported in the literature;¹⁸ among these, in one case an aminocarbene moiety is present.¹⁹ Moreover, several four-membered metallacycles of type **IV** are known,²⁰ and the examples include one iron complex.²¹ Regarding the six-membered metallacycle moiety **III**, the Fe(1)–C(13) (1.9764(18) Å) interaction is essentially a pure Fe–C(sp²) interaction, as found in related metallacycles,²² and C(13)–N(1) (1.288(2) Å) retains a double-bond character, in agreement with the presence of a metalated imino group. Similarly, the Fe(1)–N(3) distance (2.0047(16) Å) is in agreement with a σ Fe–N(sp²) interaction²³ and also C(29)–N(3) (1.285(2) Å) is essentially a double bond, indicating that also this group possesses an imino character. C(13)–C(22) (1.503(2) Å) and C(25)–C(29) (1.479(2) Å) are almost pure single bonds, whereas the C(22)–C(25) (1.360(2)

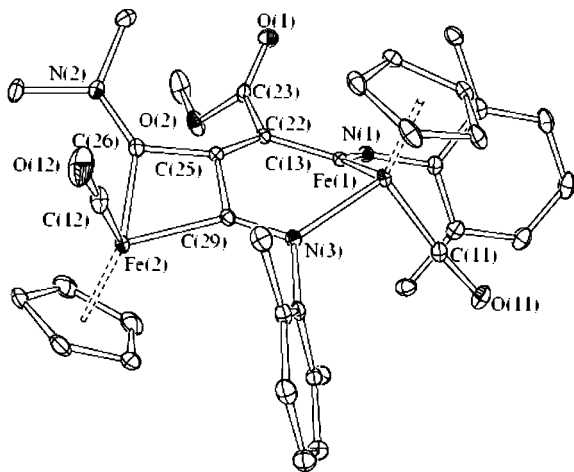


Figure 3. Molecular structure of **3**, with key atoms labeled. Displacement ellipsoids are shown at the 30% probability level. All H atoms have been omitted for clarity.

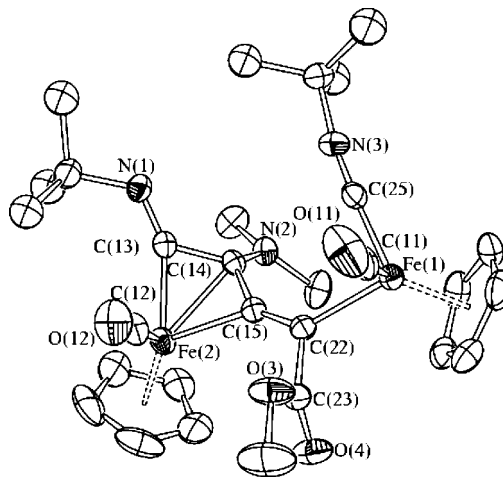


Figure 4. Molecular structure of **4**, with key atoms labeled. Displacement ellipsoids are shown at the 30% probability level. All H atoms have been omitted for clarity. Only the main images of the two disordered Bu^t groups are depicted.

Table 2. Selected Bond Lengths (Å) and Angles (deg) for **3**

Fe(1)–C(11)	1.743(2)	Fe(2)–C(12)	1.745(2)
Fe(1)–C(13)	1.9764(18)	Fe(2)–C(26)	1.898(2)
Fe(1)–N(3)	2.0047(16)	Fe(2)–C(29)	1.9409(18)
C(13)–N(1)	1.288(2)	C(11)–O(11)	1.158(2)
C(13)–C(22)	1.503(2)	C(12)–O(12)	1.149(3)
C(22)–C(25)	1.360(2)	C(25)–C(26)	1.465(2)
C(25)–C(29)	1.479(2)	C(26)–N(2)	1.302(2)
C(22)–C(23)	1.497(2)	C(29)–N(3)	1.285(2)
C(13)–Fe(1)–N(3)	90.37(7)	C(22)–C(25)–C(26)	134.97(17)
C(22)–C(13)–Fe(1)	114.69(12)	C(26)–C(25)–C(29)	97.63(14)
C(25)–C(22)–C(13)	121.67(16)	C(25)–C(26)–Fe(2)	95.09(12)
C(22)–C(25)–C(29)	123.63(16)	C(26)–Fe(2)–C(29)	70.51(8)
N(3)–C(29)–C(25)	123.23(16)	C(25)–C(29)–Fe(2)	92.86(11)
C(29)–N(3)–Fe(1)	121.30(12)	N(3)–C(29)–Fe(2)	143.65(14)

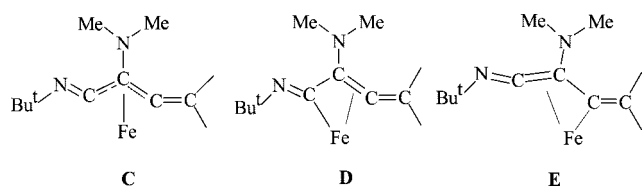
Table 3. Selected Bond Lengths (Å) and Angles (deg) for **4**

Fe(1)–C(11)	1.739(4)	C(15)–C(22)	1.309(5)
Fe(1)–C(25)	1.825(4)	C(13)–N(1)	1.261(4)
Fe(1)–C(22)	2.014(3)	C(13)–C(14)	1.455(5)
Fe(2)–C(15)	2.010(3)	C(14)–N(2)	1.368(4)
Fe(2)–C(13)	1.965(4)	C(14)–C(15)	1.417(5)
Fe(2)–C(14)	2.174(3)	C(22)–C(23)	1.484(5)
Fe(2)–C(12)	1.721(4)	C(11)–O(11)	1.140(5)
C(25)–N(3)	1.147(5)	C(12)–O(12)	1.153(5)
C(25)–Fe(1)–C(22)	91.93(15)	C(13)–Fe(2)–C(15)	72.94(14)
N(1)–C(13)–C(14)	128.1(3)	C(14)–C(13)–Fe(2)	77.3(2)
C(15)–C(14)–C(13)	110.7(3)	N(3)–C(25)–Fe(1)	176.9(4)
N(2)–C(14)–C(13)	121.8(3)	C(22)–C(15)–C(14)	144.6(3)
N(2)–C(14)–C(15)	124.9(3)	C(22)–C(15)–Fe(2)	138.8(3)
C(15)–C(22)–Fe(1)	130.3(3)	C(14)–C(15)–Fe(2)	76.6(2)
C(14)–N(2)–C(21)	120.0(3)	C(14)–N(2)–C(20)	120.2(3)
C(21)–N(2)–C(20)	115.0(3)		

Å) interaction is typical for a double bond. Therefore, the π bonds within the ring **III** can be considered to be almost completely localized. In discussing the 1-metalla-2-amino-4-iminocyclobut-1-ene ring (**IV**), the aminocarbene nature of the Fe(2)–C(26) interaction (1.898(2) Å) is notable, supported also by the partial π bond within C(26)–N(2) (1.302(2) Å).²⁴ Conversely, the Fe(2)–C(29) interaction (1.9409(18) Å) is basically a σ bond to an imino carbon, as described above for Fe(1)–C(13). Shortening of the former compared to the latter is probably due to the more strained geometry of a four-membered ring with respect to a six-membered one (compare C(26)–Fe(2)–C(29) = 70.51(8)° vs N(3)–Fe(1)–C(13) = 90.37(7)°).

The molecular structure of **4** contains a η^3 -1-aza-3-amino-penta-1,3,4-trienyl ligand coordinated to Fe(2) and metalated

Scheme 5



by Fe(1) in the 5-position (C(22) in the crystal structure, C_γ in Scheme 4). The coordination mode of the η^3 ligand can be viewed as allyl (**C**), azabutadienyl (**D**), and ketenimine (**E**) (Scheme 5), this being reminiscent of the bridging ligands previously described for the complexes $[\text{Fe}_2\{\mu\text{-}\eta^1:\eta^3\text{-C(R)-C(R')C=N(Me)}\}(\mu\text{-CO})(\text{CO})(\text{Cp})_2]$.²⁵

Thus, C(13)–N(1) (1.261(4) Å) and C(15)–C(22) (1.309(5) Å) are localized double bonds, as expected for all three electronic structures described in Scheme 5. Fe(2) is coordinated in an allyl-like fashion to all three C atoms, even though Fe(2)–C(13) (1.965(4) Å) is considerably shorter than both Fe(2)–C(14) (2.174(5) Å) and Fe(2)–C(15) (2.010(3) Å), more in agreement with the azabutadienyl form **D**. This is further supported by the fact that C(14)–C(15) (1.417(5) Å) is significantly shorter than C(13)–C(14) (1.455(5) Å). Moreover, in agreement with the enamine nature of N(2), the C(14)–N(2) (1.368(4) Å) bond is lengthened compared to the starting iminium complex (usually in the range 1.289–1.320 Å for vinyliminium ligands),³ and N(2) displays some pyramidalization (sum of angles 355.2(5)°; distance of N(2) from the plane of the pertinent carbons 0.181(4) Å). Finally, the Fe(1)–C(22) interaction displays a pure σ -bond character (Fe(1)–C(22) = 2.014(3) Å). Coordination of Fe(1) is completed by one CO, and an isocyanide ligand, whereas that of Fe(2) is completed by one Cp and a CO.

The spectroscopic data (IR and NMR) of **3** and **4** are consistent with the structures found in the solid state. The IR spectrum of **3** (in CH_2Cl_2 solution) shows two absorptions attributed to terminal carbonyls (at 1945 and 1913 cm^{-1}) and the signals due to CO_2Me (at 1713 cm^{-1}) and $\text{C}=\text{N}$ moieties (at 1606 and 1554 cm^{-1} , respectively).

The ^1H NMR spectrum of **3** shows a resonance for each methyl of the NMe_2 group (at δ 3.71 and 3.42 ppm). Their nonequivalence, due to a partial double-bond character of the C–N interaction, is in agreement with the aminocarbene character of the $\text{Fe}-\text{C}_\alpha\text{NMe}_2$ moiety, which is further evidenced

by the ^{13}C NMR resonance of C_α at 245.5 ppm. The chemical shifts of C_γ and C_β are characteristic for olefinic carbons and fall at 116.3 and 68.4 ppm, respectively, whereas the resonances attributable to the imine carbons ($>\text{CNXyl}$) are found at 157.1 and 154.0 ppm.

The IR spectrum of **4** exhibits absorptions attributed to the terminal isocyanide (at 2136 cm^{-1}), the terminal carbonyls (at 1947 cm^{-1}), and the CO_2Me group (at 1680 cm^{-1}). In the ^1H NMR spectrum of **4** the NMe_2 protons give rise to a singlet signal (δ 2.62 ppm). The equivalence of the methyls is due to free rotation around the $\text{C}_\alpha\text{-N}$ bond. Finally, the ^{13}C NMR spectrum of **4** exhibits the resonance of C_α (at 65.5 ppm) and those due to C_γ and C_β , in the downfield range typical of olefinic carbons (at 192.8 and 129.0 ppm, respectively).

The different outcomes of the reactions illustrated in Scheme 4, with respect to the formation of the ketenimine–bis(alkylidene) complexes **2a–d**, deserve some comments. Both **3** and **4** are the result of the addition or insertion of two isocyanide molecules, which produces the fragmentation of the Fe–Fe bond. An obvious consideration is that the observed differences are associated with the variation of the reaction stoichiometry. However, even when **1d** was treated with an equimolar amount of CNXyl or CNBu^t , the expected ketenimine products were not obtained. On the other hand, reactions of **1a–c** with an excess of isocyanide did not afford any multiple addition products. Therefore, the observed dissimilar reactivity is possibly related to the different nature of the bridging vinyliminium ligand in **1d** compared to that in **1a–c**: the former contains a methyl group in place of Xyl as the iminium substituent. It has been previously shown that the Xyl group, but not the CH_3 group, makes the iminium carbon hardly accessible to nucleophilic addition, for steric reasons.^{5,6} Thus, in the absence of steric protection provided by the Xyl group, the C_α position of **1d** should become available to isocyanide insertion and intramolecular rearrangements, which ultimately afford the observed products.

A common feature of the reactions leading to **3** and **4** is that the bridging vinyliminium ligand remains almost intact, in spite of the relevant intramolecular transformations. Therefore, the uncleaved $\text{Me}_2\text{N}-\text{C}_\alpha-\text{C}_\beta-\text{C}_\gamma-\text{COOMe}$ sequence can be easily recognized in both **3** and **4**, although the coordination mode and the way in which the isocyanide has inserted are, obviously, different.

Ligand Substitution by Isocyanides. In addition to ligand addition and migratory insertion, isocyanides often react via ligand substitution. This possibility takes place also in the reactions of the vinyliminium complexes shown in Scheme 6, which add a further piece of information to the general picture.

The vinyliminium complex **1e** reacts with CNBu^t , in the presence of NaH , affording after workup the dinuclear aminocarbene complexes **5** and **6**, in about 65 and 20% yields, respectively. It should be noted that the vinyliminium complex **1e** has not been previously reported. Therefore, its synthesis and properties are detailed in the Experimental Section.

The spectroscopic properties of **5** are similar to those of analogous complexes of the type $[\text{Fe}_2(\mu\text{-CNMe}_2)(\mu\text{-CO})(\text{CNR})(\text{CO})(\text{Cp})_2][\text{SO}_3\text{CF}_3]$ previously reported.²⁶ The most characteristic feature is the downfield ^{13}C NMR resonance due to the aminocarbene carbon (at δ 323.0 ppm).

(18) (a) Palm, L. H.; van Koten, G.; Vrieze, K.; Stam, C. H.; van Tunen, W. C. *J. Chem. Soc., Chem. Commun.* **1983**, 1177. (b) Rodriguez, G.; Graham, J. P.; Cotter, W. D.; Sperry, C. K.; Bazan, G. C.; Bursten, B. E. *J. Am. Chem. Soc.* **1998**, *120*, 12512. (c) van Arkel, B.; van der Baan, J. L.; Balt, S.; Bickelhaunt, F.; de Bolster, M. W. G.; Kingma, J. E.; Klumpp, G. W.; Moos, J. W. E.; Spek, A. L. *J. Chem. Soc., Perkin Trans. 1* **1993**, 3023. (d) Zahn, I.; Wagner, B.; Polborn, K.; Beck, W. *J. Organomet. Chem.* **1990**, *601*, 394. (e) Adams, H.; Bailey, N. A.; Tattershall, C. E.; Winter, M. J. *J. Chem. Soc., Chem. Commun.* **1991**, 912.

(19) Tomaszewski, R.; Arif, A. M.; Ernst, R. D. *J. Chem. Soc., Dalton Trans.* **1999**, 1883.

(20) (a) Stella, S.; Floriani, C.; Chiesi-Villa, A.; Guastini, C. *Angew. Chem., Int. Ed. Engl.* **1987**, *26*, 68. (b) Adams, R. D.; Hin, G. C. *J. Organometallics* **1991**, *10*, 1278. (c) Adams, R. D.; Hin, G. C. *J. Organometallics* **1992**, *11*, 1873.

(21) Cabrera, E.; Daran, J. C.; Jeannin, Y. *Organometallics* **1989**, *8*, 1811.

(22) Busetto, L.; Marchetti, F.; Zacchini, S.; Zanotti, V.; Zoli, E. *J. Organomet. Chem.* **2005**, *690*, 1959.

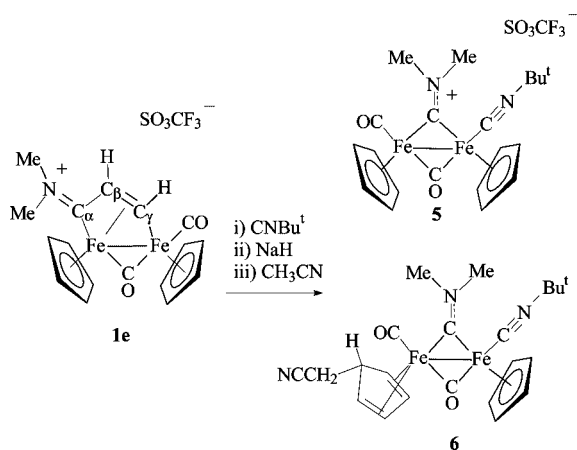
(23) (a) Busetto, L.; Marchetti, F.; Zacchini, S.; Zanotti, V.; Zoli, E. *J. Organomet. Chem.* **2005**, *690*, 348. (b) Busetto, L.; Marchetti, F.; Zacchini, S.; Zanotti, V. *Inorg. Chim. Acta* **2005**, *358*, 1204.

(24) Busetto, L.; Zanotti, V. *J. Organomet. Chem.* **2005**, *690*, 5430.

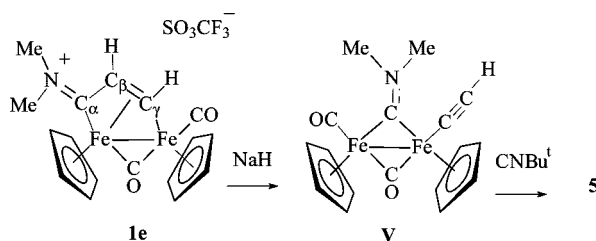
(25) Albano, V. G.; Busetto, L.; Marchetti, F.; Monari, M.; Zacchini, S.; Zanotti, V. *Organometallics* **2007**, *26*, 3448.

(26) (a) Boss, K.; Dowling, C.; Manning, A. R. *J. Organomet. Chem.* **1996**, *509*, 197. (b) Cox, G.; Dowling, C.; Manning, A. R.; McArdle, P.; Cunningham, D. *J. Organomet. Chem.* **1992**, *438*, 143. (c) Willis, S.; Manning, A. R.; Stephens, F. S. *J. Chem. Soc., Dalton Trans.* **1980**, 186.

Scheme 6



Scheme 7



The formation of **5** is the consequence of acetylene deinsertion from the bridging vinyliminium ligand in **1e**, which presumably proceeds through the acetylide intermediate **V** (Scheme 7). This hypothesis is consistent with the fact that a number of vinyliminium complexes, such as $[\text{Fe}_2\{\mu\text{-}\eta^1\text{-}\eta^3\text{-C}_\gamma(\text{R}')\text{C}_\beta(\text{H})\text{C}_\alpha\text{N}(\text{Me})\text{R}\}\text{-}(\mu\text{-CO})(\text{CO})(\text{Cp})_2][\text{SO}_3\text{CF}_3]$ ($\text{R} = \text{Xyl}, \text{Me}$; $\text{R}' = \text{Tol}, \text{SiMe}_3$), are known to be transformed into acetylide complexes analogous to **V**, upon treatment with NaH.⁸ Therefore, complex **5** should result from acetylide replacement by isocyanide.

The formation of **6** is more difficult to explain. It presumably derives from **5** via addition of the NCCH_2^- carbanion to the Cp ligand. This step might occur during the chromatography on alumina, since CH_3CN , used as eluent, might come in contact with NaH and generate the cyanomethanide anion. Analogous additions of carbanionic reagents to the Cp ring of dinuclear μ -aminocarbyne complexes have been previously reported.²⁷ These nucleophilic additions are known to produce stable dinuclear cyclopentadiene complexes similar to **6**.²⁷

Complex **6** was spectroscopically characterized, and its molecular structure has been elucidated by X-ray diffraction (Figure 5 and Table 4). The molecule comprises a diiron frame bonded to a bridging and a terminal CO, a terminal isonitrile, a bridging aminocarbyne, one η^5 -Cp, and a η^4 -cyclopentadiene ligand. Bonding parameters are in keeping with those previously reported for analogous complexes.^{26–28}

The IR spectrum of **6** (in CH_2Cl_2 solution) shows the usual $\nu(\text{CO})$ band pattern, consisting of two absorptions (at 1915 and 1751 cm^{-1}), and two $\nu(\text{CN})$ absorptions (at 2107 and 2070 cm^{-1}). In comparison to **5**, the $\nu(\text{CO})$ absorptions are shifted to lower frequencies, as a consequence of the fact that **6** is

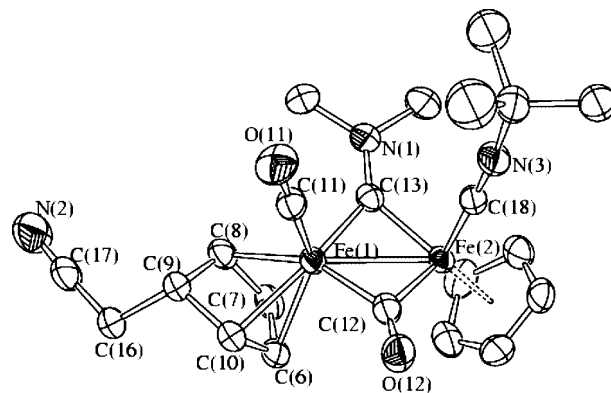


Figure 5. Molecular structure of **6**, with key atoms labeled. Displacement ellipsoids are shown at the 30% probability level. All H atoms have been omitted for clarity. Only the main image of the two disordered Bu^t groups is depicted.

Table 4. Selected Bond Lengths (Å) and Angles (deg) for **6**

Fe(2)–Fe(1)	2.5262(5)	Fe(1)–C(6)	2.060(3)
Fe(1)–C(11)	1.755(3)	Fe(1)–C(7)	2.048(3)
Fe(1)–C(12)	1.887(3)	Fe(1)–C(8)	2.120(3)
Fe(2)–C(12)	1.963(3)	Fe(1)–C(10)	2.151(2)
Fe(1)–C(13)	1.852(2)	C(6)–C(7)	1.409(4)
Fe(2)–C(13)	1.878(3)	C(6)–C(10)	1.396(4)
Fe(2)–C(18)	1.814(3)	C(7)–C(8)	1.418(4)
C(13)–N(1)	1.305(3)	C(8)–C(9)	1.506(4)
C(18)–N(3)	1.154(3)	C(9)–C(10)	1.503(4)
C(11)–O(11)	1.142(3)	C(9)–C(16)	1.566(4)
C(12)–O(12)	1.176(3)	C(16)–C(17)	1.433(5)
Fe(2)–Ct	1.740(2)	C(17)–N(2)	1.133(5)
N(3)–C(18)–Fe(2)	178.6(3)	C(7)–C(8)–C(9)	109.0(3)
Fe(1)–C(13)–Fe(2)	85.25(11)	C(10)–C(9)–C(8)	96.1(2)
N(1)–C(13)–Fe(2)	136.3(2)	C(6)–C(10)–C(9)	109.3(3)
N(1)–C(13)–Fe(1)	138.1(2)	C(10)–C(6)–C(7)	107.9(2)
Fe(1)–C(12)–Fe(2)	81.99(12)	C(17)–C(16)–C(9)	110.6(3)
C(6)–C(7)–C(8)	106.4(2)	N(2)–C(17)–C(16)	175.9(4)

neutral, whereas **5** is cationic. The NMR spectra indicate the presence in solution of a single isomer, which presumably assumes the same configuration found in the solid state. The geminal hydrogen atoms of the cyanomethyl group give rise to a single resonance at 1.56 ppm, whereas the two *N*-methyl groups exhibit distinct resonances, due to their nonequivalence and to the double-bond character of the $\mu\text{-C}=\text{N}$ interaction. Finally, in the ^{13}C NMR spectrum is observed the typical low-field resonance of the aminocarbyne carbon (at 330.3 ppm).

Conclusions

Our investigations revealed new possible transformations of the bridging vinyliminium ligand by reactions with isocyanides, in the presence of NaH as proton abstractor. Three distinct reaction routes were evidenced: (i) isocyanide addition at the vinyliminium ligand, (ii) multiple isocyanide addition, and (iii) ligand substitution. Relevant features for each type of reactivity pattern are the following:

(i) The addition of isocyanides to the central carbon of the C_3 bridging unit generates a ketenimine functional group. The result is remarkable, in that a $\text{C}_\beta\text{-H}$ bond is replaced with a $\text{C}=\text{C}$ double bond. This transformation is made possible by a change in the coordination mode of the bridging fragment: the C_β carbon is released from metal coordination, whereas the other two carbon atoms of the C_3 -bridged frame assume a more distinct alkylidene character.

(ii) In the absence of the Xyl group, which exerts some steric “protection”, the vinyliminium ligand is involved in multiple

(27) Albano, V. G.; Busetto, L.; Camiletti, C.; Castellari, C.; Monari, M.; Zanotti, V. *J. Chem. Soc., Dalton Trans.* **1997**, 4671.

(28) (a) Boss, K.; Cox, M. G.; Dowling, C.; Manning, A. R. *J. Organomet. Chem.* **2000**, 612, 18. (b) Albano, V. G.; Busetto, L.; Marchetti, F.; Monari, M.; Zanotti, V. *J. Organomet. Chem.* **2002**, 649, 64. (c) Busetto, L.; Marchetti, F.; Zacchini, S.; Zanotti, V. *Inorg. Chim. Acta* **2005**, 358, 1204. (d) Albano, V. G.; Busetto, L.; Marchetti, F.; Monari, M.; Zacchini, S.; Zanotti, V. *Z. Naturforsch., B* **2007**, 427.

Table 5. Crystal Data and Experimental Details for 2a,b, 3·1.5CH₂Cl₂, 4, and 6·0.5Et₂O

	2a	2b	3·1.5CH ₂ Cl ₂	4	6·0.5Et ₂ O
formula	C ₃₄ H ₃₄ Fe ₂ N ₂ O ₂	C ₃₅ H ₃₄ Fe ₂ N ₂ O ₂	C _{38.5} H ₄₀ Cl ₃ Fe ₂ N ₃ O ₄	C ₂₉ H ₃₇ Fe ₂ N ₃ O ₄	C ₂₄ H ₃₂ Fe ₂ N ₃ O _{2.5}
fw	614.33	658.34	826.79	603.32	514.23
T, K	293(2)	293(2)	100(2)	296(2)	293(2)
λ, Å	0.710 73	0.710 73	0.710 73	0.710 73	0.710 73
cryst syst	monoclinic	monoclinic	triclinic	monoclinic	monoclinic
space group	P2 ₁ /c	P2 ₁ /c	P $\bar{1}$	P2 ₁ /c	C2/c
a, Å	15.125(3)	13.849(3)	11.013(2)	12.595(3)	30.013(3)
b, Å	12.884(3)	13.765(3)	11.506(2)	16.987(3)	14.6744(17)
c, Å	15.943(3)	17.266(4)	14.818(3)	15.355(3)	11.5698(13)
α, deg	90	90	94.56(3)	90	90
β, deg	106.24(3)	112.71(3)	93.89(3)	112.73(3)	99.670(2)
γ, deg	90	90	95.94(3)	90	90
V, Å ³	2982.7(10)	3036.4(11)	1856.1(6)	3030.1(11)	5023.1(10)
Z	4	4	2	4	8
D _c , g cm ⁻³	1.368	1.440	1.479	1.323	1.360
μ, mm ⁻¹	1.005	0.998	1.042	0.993	1.181
F(000)	1280	1368	854	1264	2152
cryst size, mm	0.23 × 0.18 × 0.12	0.26 × 0.21 × 0.16	0.34 × 0.28 × 0.19	0.28 × 0.23 × 0.16	0.22 × 0.19 × 0.14
θ limits, deg	1.40–27.10	1.59–27.48	1.38–27.10	1.75–25.55	1.38–26.37
no. of rflns collected	30 871	32 638	19 454	27 820	26 607
no. of indep rflns	6585 (R _{int} = 0.0744)	6961 (R _{int} = 0.0576)	8185 (R _{int} = 0.0317)	5679 (R _{int} = 0.0632)	5129 (R _{int} = 0.0256)
no. of data/restraints/params	6585/72/362	6961/3/414	8185/28/474	5679/222/354	5129/80/312
goodness on fit on F ²	1.025	1.050	1.028	1.071	1.077
R1 (I > 2σ(I))	0.0509	0.0419	0.0373	0.0506	0.0362
wR2 (all data)	0.142 66	0.1203	0.0914	0.1537	0.1154
largest diff peak/hole, e Å ⁻³	0.626/–0.589	0.966/–0.423	0.673/–0.898	0.569/–0.478	0.341/–0.313

isocyanide addition/insertion and rearrangement reactions. These result in the cleavage of the Fe–Fe bond and formation of novel bridging organic frames, with rather complicated, and hardly predictable, molecular architectures.

(iii) For some vinyliminium complexes C_β–H deprotonation produces acetylde deinsertion. In these cases isocyanide acts as the ligand, displacing acetylde and coordinating one metal center.

Isocyanide addition at the bridging vinyliminium ligand is consistent with the reactivity pattern previously observed and described in Scheme 1. Conversely, reactions leading to multiple isocyanide addition, insertion, intramolecular rearrangement, or ligand substitution appear erratic and rather unpredictable; the corresponding products are complex and mostly unexpected. The observed variety of reaction products accounts for the flexibility of the vinyliminium ligand and the various coordination modes provided by the diiron frame, in combination with the huge potential that isocyanides offer as reagents.

Experimental Section

General Data. All reactions were routinely carried out under a nitrogen atmosphere, using standard Schlenk techniques. Solvents were distilled immediately before use under nitrogen from appropriate drying agents. Chromatography separations were carried out on columns of deactivated alumina (4% w/w water). Glassware was oven-dried before use. Infrared spectra were recorded at 298 K on a Perkin-Elmer Spectrum 2000 FT-IR spectrophotometer, and elemental analyses were performed on a ThermoQuest Flash 1112 Series EA instrument. ESI MS spectra were recorded on a Waters Micromass ZQ 4000 with samples dissolved in CH₃CN. All NMR measurements were performed on a Varian Mercury Plus 400 instrument. The chemical shifts for ¹H and ¹³C were referenced to internal TMS. The spectra were fully assigned via DEPT experiments and ¹H, ¹³C correlation measured through gs-HSQC and gs-HMBC experiments.²⁹ Unless otherwise stated, NMR spectra were recorded at 298 K; NMR signals due to a second isomeric form (where it has been possible to detect and/or resolve them) are italicized. NOE measurements were recorded using the DPFGSE-NOE sequence.³⁰ All reagents were commercial products (Aldrich) of the highest purity available and were used as received.

[Fe₂(CO)₄(Cp)₂] was purchased from Strem and used as received. Compounds **1a**,^{3a} **1b**,^{3b} **1c**,⁷ and [Fe₂{μ-CN(Me)₂}(Cp)₂(μ-CO)(CO)(Cl)]³¹ were prepared by published methods.

Synthesis of [Fe₂{μ-η¹:η³-C_γ(H)C_β(H)C_αN(Me)₂}(μ-CO)(CO)(Cp)₂][SO₃CF₃] (1e**).** Acetylene was bubbled for about 1 min into a solution of the complex [Fe₂{μ-CN(Me)₂}(Cp)₂(μ-CO)(CO)(Cl)] (150 mg, 0.284 mmol) in CH₂Cl₂ (20 mL). Then, AgSO₃CF₃ (80 mg, 0.312 mmol) was added to the solution and the resulting mixture was stirred for 30 min. Removal of solvent and chromatography of the residue on an alumina column with MeOH as eluent gave a brown band corresponding to **1e**. The product was obtained as a microcrystalline powder upon removal of the solvent under reduced pressure. Yield: 126 mg, 84%. Anal. Calcd for C₁₈H₁₈F₃Fe₂NO₅S: C, 40.86; H, 3.43; N, 2.65. Found: C, 40.96; H, 3.35; N, 2.71. IR (CH₂Cl₂): ν(CO) 1994 (vs), 1816 (s), ν(C=N) 1676 (w) cm⁻¹. ¹H NMR (CDCl₃): 12.37 (d, 1 H, ³J_{HH} = 7 Hz, C_γH); 5.51, 5.18 (s, 10 H, Cp); 4.30 (d, 1 H, ³J_{HH} = 7 Hz, C_βH); 3.92, 3.34 ppm (s, 6 H, NMe). ¹³C{¹H} NMR (CDCl₃): 226.7 (C_α); 202.5 (C_γ); 89.7, 86.9 (Cp); 51.9 (C_β); 50.0, 44.0 ppm (NMe).

Synthesis of [Fe₂{μ-η¹:η²-C_γ(R')C_β(CNR'')C_αN(Me)(R)}(μ-CO)(CO)(Cp)₂] (R = Xyl, R' = Me, R'' = Xyl, **2a; R = Xyl, R' = CO₂Me, R'' = Xyl, **2b**; R = Xyl, R' = CO₂Me, R'' = Bu^t, **2c**; R = Xyl, R' = CO₂Me, R'' = 4-C₆H₄CN, **2d**; R = 4-C₆H₄OMe, R' = CO₂Me, R'' = Bu^t, **2e**).** A solution of **1a** (189 mg, 0.299 mmol), in THF (20 mL), was treated with CNXyl (196 mg, 1.50 mmol) and then with NaH (57 mg, 2.38 mmol). The mixture, which turned orange, was stirred for 60 min and filtered on an alumina pad. Solvent removal gave a residue that was chromatographed on an alumina column. Elution with a 1:2 mixture of CH₂Cl₂ and Et₂O as eluent gave an orange band corresponding to **2a**. Yield: 108 mg, 59%. Crystals suitable for X-ray diffraction were collected from a CH₂Cl₂ solution layered with petroleum ether (bp 40–60 °C), at –20 °C. Anal. Calcd for C₃₄H₃₄Fe₂N₂O₂: C, 66.47; H, 5.58; N, 4.56. Found: C, 66.43; H, 5.51; N, 4.55. IR (CH₂Cl₂): ν(C=C=N) 1962 (m), ν(CO) 1919 (vs), 1730 (s), ν(CN)

(29) Wilker, W.; Leibfritz, D.; Kerssebaum, R.; Beimele, W. *Magn. Reson. Chem.* **1993**, *31*, 287.

(30) Stott, K.; Stonehouse, J.; Keeler, J.; Hwang, T. L.; Shaka, A. J. *J. Am. Chem. Soc.* **1995**, *117*, 4199.

(31) Albano, V. G.; Busetto, L.; Monari, M.; Zanotti, V. *J. Organomet. Chem.* **2000**, *606*, 163.

1505 (m) cm^{-1} . ^1H NMR (CDCl_3): 7.22–6.50 (m, 6 H, $\text{Me}_2\text{C}_6\text{H}_3$), 4.64, 4.51 (s, 10 H, Cp), 3.52, (s, 3 H, NMe), 3.44 (s, 3 H, C_γMe), 2.17, 1.83 (s, 6 H, $\text{C}_\alpha\text{NC}_6\text{H}_3\text{Me}_2$), 2.05 ppm (s, 6 H, $\text{C}_\beta\text{CNC}_6\text{H}_3\text{Me}_2$). $^{13}\text{C}\{^1\text{H}\}$ NMR (CDCl_3): 282.7 ($\mu\text{-CO}$), 241.2 (C_α), 218.0 (CO), 156.1 (C_γ), 148.0 (C_βCN), 146.3 (*ipso*- $\text{Me}_2\text{C}_6\text{H}_3$), 142.2 (*ipso*- $\text{Me}_2\text{C}_6\text{H}_3$), 133.7–127.7 ($\text{C}_6\text{H}_3\text{Me}_2$), 99.0 (C_β), 86.2, 85.4 (Cp), 45.4 (NMe), 41.4 (C_γMe), 18.9 ($\text{C}_\beta\text{CNMe}_2\text{C}_6\text{H}_3$), 17.8 ($\text{C}_\alpha\text{NMe}_2\text{C}_6\text{H}_3$), 17.0 ppm ($\text{C}_\alpha\text{NMe}_2\text{C}_6\text{H}_3$).

Compounds **2b–e** were prepared by the same procedure described for **2a**, by reacting **1b,c** with the appropriate isocyanide and NaH.

2b (yield 68%; orange). Anal. Calcd for $\text{C}_{35}\text{H}_{34}\text{Fe}_2\text{N}_2\text{O}_4$: C, 63.85; H, 5.21; N, 4.26. Found: C, 63.92; H, 5.17; N, 4.19. IR (CH_2Cl_2): $\nu(\text{C}=\text{C}=\text{N})$ 2024 (m), $\nu(\text{CO})$ 1931 (vs), 1746 (s), 1661 (w), $\nu(\text{CN})$ 1505 (m) cm^{-1} . ^1H NMR (CDCl_3): 7.00–6.41 (m, 6 H, $\text{Me}_2\text{C}_6\text{H}_3$); 4.69, 4.62 (s, 10 H, Cp); 3.83 (s, 3 H, CO_2Me); 3.46 (s, 3 H, NMe); 2.13, 1.89 (s, 6 H, $\text{C}_\alpha\text{NC}_6\text{H}_3\text{Me}_2$); 2.09 ppm (s, 6 H, $\text{C}_\beta\text{CNC}_6\text{H}_3\text{Me}_2$). $^{13}\text{C}\{^1\text{H}\}$ NMR (CDCl_3): 277.0 ($\mu\text{-CO}$); 234.9 (C_α); 217.3 (CO); 182.2 (CO_2Me); 142.4 (*ipso*- $\text{Me}_2\text{C}_6\text{H}_3$); 137.4 (*ipso*- $\text{Me}_2\text{C}_6\text{H}_3$); 136.0 (C_βCN); 133.6, 133.3, 128.3, 128.1, 127.9, 127.7, 127.6 ($\text{Me}_2\text{C}_6\text{H}_3$); 131.4 (C_γ); 95.5 (C_β); 86.2, 86.0 (Cp); 50.5 (CO_2Me); 45.0 (NMe); 18.8 ($\text{C}_\beta\text{CNC}_6\text{H}_3\text{Me}_2$); 17.9, 17.0 ppm ($\text{Me}_2\text{C}_6\text{H}_3$).

2c (yield 70%; orange). Anal. Calcd for $\text{C}_{31}\text{H}_{34}\text{Fe}_2\text{N}_2\text{O}_4$: C, 61.01; H, 5.62; N, 4.59. Found: C, 60.98; H, 5.70; N, 4.56. IR (CH_2Cl_2): $\nu(\text{C}=\text{C}=\text{N})$ 1989 (vs), (CO) 1931 (vs), 1745 (s), 1661 (m), ($\text{C}=\text{N}$) 1512 (m) cm^{-1} . ^1H NMR (CDCl_3): 7.03–6.87 (m, 3 H, $\text{Me}_2\text{C}_6\text{H}_3$); 4.64, 4.58 (s, 10 H, Cp); 3.86 (s, 3 H, CO_2Me); 3.43 (s, 3 H, NMe); 2.05, 1.85 (s, 6 H, $\text{Me}_2\text{C}_6\text{H}_3$); 0.84 ppm (s, 9 H, Bu^t). $^{13}\text{C}\{^1\text{H}\}$ NMR (CDCl_3): 277.5 ($\mu\text{-CO}$); 239.1 (C_α); 217.4 (CO); 181.9 (CO_2Me); 143.1 (C_βCN); 141.7 (*ipso*- $\text{Me}_2\text{C}_6\text{H}_3$); 134.4, 133.4, 128.9, 128.4, 128.1 ($\text{Me}_2\text{C}_6\text{H}_3$); 123.8 (C_γ); 96.3 (C_β); 86.4, 86.1 (Cp); 60.3 (CMe_3); 50.3 (CO_2Me); 46.1 (NMe); 29.9 (CMe_3); 17.7, 16.9 ppm ($\text{Me}_2\text{C}_6\text{H}_3$).

2d (yield 69%; brown). Anal. Calcd for $\text{C}_{34}\text{H}_{29}\text{Fe}_2\text{N}_3\text{O}_4$: C, 62.32; H, 4.46; N, 6.41. Found: C, 62.38; H, 4.39; N, 6.44. IR (CH_2Cl_2): $\nu(\text{C}\equiv\text{N})$ 2219 (m), $\nu(\text{C}=\text{C}=\text{N})$ 2024 (m), $\nu(\text{CO})$ 1938 (vs), 1747 (s), 1665 (m), $\nu(\text{C}=\text{N})$ 1515 (m) cm^{-1} . ^1H NMR (CDCl_3): 7.38, 7.28, 6.64, 6.20 (d, 2 H, $^3J_{\text{HH}} = 8.5$ Hz, $\text{C}_6\text{H}_4\text{CN}$); 7.12–6.99 (m, 3 H, $\text{Me}_2\text{C}_6\text{H}_3$); 4.70, 4.62 (s, 10 H, Cp); 3.93 (s, 3 H, CO_2Me); 3.56 (s, 3 H, NMe); 2.05, 1.86 ppm (s, 6 H, $\text{Me}_2\text{C}_6\text{H}_3$). $^{13}\text{C}\{^1\text{H}\}$ NMR (CDCl_3): 276.0 ($\mu\text{-CO}$); 242.9 (C_α); 217.3 (CO); 185.0 (CO_2Me); 145.6, 145.3 (*ipso*- $\text{C}_6\text{H}_4\text{CN}$ and C_βCN); 140.5 (*ipso*- $\text{Me}_2\text{C}_6\text{H}_3$); 133.2, 117.1, 114.3, 114.0 ($\text{C}_6\text{H}_4\text{CN}$); 132.8, 132.7, 129.5, 129.3, 128.3 ($\text{Me}_2\text{C}_6\text{H}_3$); 124.7 (C_γ); 119.6 ($\text{C}\equiv\text{N}$); 102.1 (C_β); 86.8, 85.9 (Cp); 50.9 (CO_2Me); 46.6 (NMe); 17.6, 16.7 ppm ($\text{Me}_2\text{C}_6\text{H}_3$).

2e (yield 65%; orange). Anal. Calcd for $\text{C}_{30}\text{H}_{32}\text{Fe}_2\text{N}_2\text{O}_5$: C, 58.85; H, 5.27; N, 4.58. Found: C, 58.92; H, 5.24; N, 4.63. IR (CH_2Cl_2): $\nu(\text{C}=\text{C}=\text{N})$ 2126 (m), $\nu(\text{CO})$ 1954 (vs), 1765 (s), 1692 (w) cm^{-1} . ^1H NMR (CDCl_3): 7.26–6.58 (m, 4 H, $\text{C}_6\text{H}_4\text{OMe}$); 4.68, 4.53 (s, 10 H, Cp); 3.80 (s, 3 H, CO_2Me); 3.75 (s, 3 H, OMe); 3.33 (s, 3 H, NMe); 1.20 ppm (s, 9 H, Bu^t). $^{13}\text{C}\{^1\text{H}\}$ NMR (CDCl_3): 286.2 ($\mu\text{-CO}$); 235.4 (C_α); 231.2 (CO); 183.3 (CO_2Me); 160.4 (*ipso*- C_6H_4); 140.2–113.5 (C_6H_4 and C_γ); 133.6 (C_βCN); 98.4 (C_β); 90.4, 89.5 (Cp); 55.8 (CO_2Me); 52.0 (OMe); 40.9 ppm (NMe).

Synthesis of $[\text{Fe}(\text{CO})(\text{Cp})\text{C}_\alpha(\text{NMe}_2)\text{C}_\beta(\text{CNXyl})\text{C}_\gamma(\text{CO}_2\text{Me})\text{C}(\text{NXyl})\text{Fe}(\text{CO})(\text{Cp})]$ (3**).** A solution of **1d** (225 mg, 0.385 mmol), in THF (20 mL), was treated with CNXyl (200 mg, 1.53 mmol) and then with NaH (45 mg, 1.88 mmol). The mixture was stirred for 90 min, and then it was filtered on alumina. Solvent removal and chromatography of the residue on an alumina column with THF as eluent gave a green band corresponding to **3**. Yield: 188 mg, 70%. Crystals suitable for X-ray diffraction were collected from a CH_2Cl_2 solution layered with *n*-pentane, at -20 °C. Anal. Calcd for $\text{C}_{37}\text{H}_{37}\text{Fe}_2\text{N}_3\text{O}_4$: C, 63.54; H, 5.33; N, 6.01. Found: C, 63.58; H, 5.29; N, 5.90. IR (CH_2Cl_2): $\nu(\text{CO})$ 1945 (s), 1913 (vs), 1713

(w), $\nu(\text{C}=\text{N})$ 1606 (w), 1554 (w) cm^{-1} . ^1H NMR (CDCl_3): 7.07–6.77 (m, 6 H, $\text{Me}_2\text{C}_6\text{H}_3$); 4.19, 4.16 (s, 10 H, Cp); 3.71 (s, 3 H, CO_2Me); 3.71, 3.42 (s, 6 H, NMe); 2.28, 2.23 (s, 6 H, $\text{Me}_2\text{C}_6\text{H}_3$); 2.08 ppm (s, 6 H, $\text{Me}_2\text{C}_6\text{H}_3$). $^{13}\text{C}\{^1\text{H}\}$ NMR (CDCl_3): 245.5 (C_α); 222.7, 220.3 (CO); 169.2 (CO_2Me); 157.1, 154.0 (CNXyl); 141.4, 140.2 (*ipso*- $\text{Me}_2\text{C}_6\text{H}_3$); 130.7–121.3 ($\text{Me}_2\text{C}_6\text{H}_3$); 116.3 (C_γ); 82.6, 82.3 (Cp); 68.4 (C_β); 51.9 (CO_2Me); 48.8, 45.3 (NMe); 20.1, 19.3, 18.9, 18.3 ppm ($\text{Me}_2\text{C}_6\text{H}_3$).

Synthesis of $[\text{Fe}(\text{CO})(\text{Cp})\text{C}(\text{NBU}^t)\text{C}_\alpha(\text{NMe}_2)\text{C}_\beta\text{C}_\gamma(\text{CO}_2\text{Me})\text{Fe}(\text{Cp})(\text{CO})\text{CNBU}^t]$ (4**).** A solution of complex **1d** (150 mg, 0.256 mmol), in THF (20 mL), was treated with CNBU^t (1.05 mmol) and then with NaH (31 mg, 1.29 mmol). The mixture was stirred for 60 min, and then the solvent was removed under reduced pressure and the residue was chromatographed on an alumina column. A red band was collected by using a 1:2 mixture of CH_2Cl_2 and Et_2O as eluent. Yield: 100 mg, 65%. Crystals suitable for X-ray diffraction were obtained from a Et_2O solution at -20 °C. Anal. Calcd for $\text{C}_{29}\text{H}_{37}\text{Fe}_2\text{N}_3\text{O}_4$: C, 57.73; H, 6.18; N, 6.96. Found: C, 57.79; H, 6.17; N, 7.02. IR (CH_2Cl_2): $\nu(\text{C}\equiv\text{N})$ 2136 (m), (CO) 1947 (vs), 1680 (m), $\nu(\text{C}=\text{N})$ 1636 (m) cm^{-1} . ^1H NMR (CDCl_3): 4.61, 4.48 (s, 10 H, Cp); 3.79 (s, 3 H, CO_2Me); 2.62 (s, 6 H, NMe); 1.44, 1.41 ppm (s, 18 H, Bu^t). $^{13}\text{C}\{^1\text{H}\}$ NMR (CDCl_3): 218.9, 217.6 (CO); 192.8 (C_γ); 176.5 (CO_2Me); 164.3 ($\text{C}\equiv\text{NBU}^t$); 148.2 ($\text{C}=\text{NBU}^t$); 129.0 (C_β); 84.2, 80.2 (Cp); 65.5 (C_α); 57.4, 56.6 (CMe_3); 50.5 (CO_2Me); 38.6 (NMe₂); 30.9, 30.4 ppm (CMe_3).

Synthesis of $[\text{Fe}_2\{\mu\text{-CN}(\text{Me})_2\}(\mu\text{-CO})(\text{CO})(\text{CNBU}^t)(\text{Cp})_2]$ (5**) and $[\text{Fe}_2\{\mu\text{-CN}(\text{Me})_2\}(\mu\text{-CO})(\text{CO})(\text{Cp})(\text{C}_5\text{H}_5\text{CH}_2\text{CN})(\text{CNBU}^t)]$ (**6**).** A solution of **1e** (120 mg, 0.227 mmol) in THF (15 mL) was treated with NaH (139 mg, 5.79 mmol) in the presence of CNBU^t (0.50 mmol). The mixture was stirred for 30 min and then filtered on alumina, with CH_3CN as eluent. Removal of the volatile material gave a solid residue that was chromatographed on alumina, using CH_2Cl_2 as eluent. Two bands were collected. The first one, green, corresponded to **6**: yield 70 mg, 65%. Crystals of **6** suitable for X-ray analysis were collected from a diethyl ether solution layered with *n*-pentane, at -20 °C. Anal. Calcd for $\text{C}_{22}\text{H}_{27}\text{Fe}_2\text{N}_3\text{O}_2$: C, 55.38; H, 5.70; N, 8.81. Found: C, 55.43; H, 5.76; N, 8.74. IR (CH_2Cl_2): $\nu(\text{C}\equiv\text{N})$ 2107 (m), 2070 (m-sh), $\nu(\text{CO})$ 1915 (vs), 1751 (s) cm^{-1} . ^1H NMR (CDCl_3): 4.47 (s, 5 H, Cp); 4.11, 3.74, 3.65, 3.32, 3.03 (m, 5 H, $\text{C}_5\text{H}_5\text{CH}_2\text{CN}$); 3.96, 3.79 (s, 6 H, NMe); 1.56 (m, 2 H, CH_2CN); 1.20 ppm (s, 9 H, CMe_3). $^{13}\text{C}\{^1\text{H}\}$ NMR (CDCl_3): 330.3 ($\mu\text{-CN}$); 271.3 ($\mu\text{-CO}$); 213.7 (CO); 148.6 (CH_2CN); 124.6 (CNBU^t); 89.6, 87.8, 87.3, 86.6, 81.1 ($\text{C}_5\text{H}_5\text{CH}_2\text{CN}$); 88.4 (Cp); 61.0 (CH_2CN); 56.6 (CMe_3); 46.9, 46.6 (NMe₂); 31.3 ppm (CMe_3).

The second band, red, collected by using CH_3CN as eluent, corresponded to **5**: yield 27 mg, 20%. Anal. Calcd for $\text{C}_{21}\text{H}_{25}\text{F}_3\text{Fe}_2\text{N}_2\text{O}_5\text{S}$: C, 47.03; H, 4.30; N, 4.78. Found: C, 47.12; H, 4.21; N, 4.83. IR (CH_2Cl_2): $\nu(\text{C}\equiv\text{N})$ 2141 (vs), $\nu(\text{CO})$ 1985 (vs), 1806 (s), $\nu(\text{C}=\text{N})$ 1587 (m) cm^{-1} . ^1H NMR (CDCl_3): δ 5.01, 4.92 (s, 10 H, Cp); 4.57 (s, 6 H, NMe); 1.11 ppm (s, 9 H, CNCMe_3). $^{13}\text{C}\{^1\text{H}\}$ NMR (CDCl_3): δ 323.0 ($\mu\text{-C}$); 261.5 ($\mu\text{-CO}$); 210.3 (CO); 119.2 ($\text{C}\equiv\text{N}$); 88.2, 86.7 (Cp); 58.2 (CMe_3); 52.2 (NMe); 30.6 ppm (CMe_3).

X-ray Crystallography. Crystal data and collection details for **2a,b**, **3**·1.5 CH_2Cl_2 , **4**, and **6**·0.5 Et_2O are reported in Table 5. The diffraction experiments were carried out on a Bruker Apex II diffractometer (for **6**·0.5 Et_2O) and on a Bruker SMART 2000 diffractometer (for **2a,b**, **3**·1.5 CH_2Cl_2 , and **4**) equipped with a CCD detector using Mo $\text{K}\alpha$ radiation. Data were corrected for Lorentz–polarization and absorption effects (empirical absorption correction SADABS).³² Structures were solved by direct

(32) Sheldrick, G. M. SADABS, Program for Empirical Absorption Correction; University of Göttingen, Göttingen, Germany, 1996.

(33) Sheldrick, G. M. SHELX97, Program for Crystal Structure Determination; University of Göttingen, Göttingen, Germany, 1997.

methods and refined by full-matrix least squares based on all data using F^2 .³³ Non-H atoms were refined anisotropically, unless otherwise stated. H atoms were placed in calculated positions, except H(9) in **6**·0.5Et₂O, which was located in the Fourier map. H atoms were treated isotropically using the 1.2-fold U_{iso} value of the parent atom, except for methyl protons, which were assigned the 1.5-fold U_{iso} value of the parent C atom. The Xyl group in **2a**, the OMe group in **2b**, one CH₂Cl₂ molecule (located close to an inversion center) in **3**·1.5CH₂Cl₂, the two Bu^t groups in **4**, and the Bu^t group and the Et₂O molecule in **6**·0.5Et₂O are disordered. Disordered atomic positions were split and refined using one occupancy parameter per disordered group.

Acknowledgment. We thank the Ministero dell'Università e della Ricerca (MUR) (project: "New strategies for the control of reactions: interactions of molecular fragments with metallic sites in unconventional species") and the University of Bologna for financial support.

Supporting Information Available: CIF files giving crystallographic data for the compounds **2a,b**, **3**·1.5CH₂Cl₂, **4**, and **6**·0.5Et₂O. This material is available free of charge via the Internet at <http://pubs.acs.org>.

OM800445K